3D Printing Of A Cranial Implant With Energy-Absorbing Polymer Via Arburg Plastic Freeforming Technology

Published Version:
Mele, M., Cercenelli, L., Pisaneschi, G., Fiorini, M., Zucchelli, A., Campana, G., et al. (2023). 3D Printing Of A Cranial Implant With Energy-Absorbing Polymer Via Arburg Plastic Freeforming Technology. JOURNAL OF MECHANICS IN MEDICINE AND BIOLOGY, 23(6), 1-16 [10.1142/S0219519423400249].

Availability:
This version is available at: https://hdl.handle.net/11585/951969 since: 2024-01-04

Published:

DOI: http://doi.org/10.1142/S0219519423400249

Mele, M., Cercenelli, L., Pisaneschi, G., Fiorini, M., Zucchelli, A., Campana, G., Tarsitano, A. and Marcelli, E., 2023. 3D PRINTING OF A CRANIAL IMPLANT WITH ENERGY-ABSORBING POLYMER VIA ARBURG PLASTIC FREEFORMING TECHNOLOGY. Journal of Mechanics in Medicine and Biology, p.2340024.]

The final published version is available online at: **https://doi.org/10.1142/S0219519423400249**

Journal of Mechanics in Medicine and Biology

3D printing of a cranial implant with energy-absorbing polymer via Arburg Plastic Freeforming technology

--Manuscript Draft--

Manuscript Number:	JMMB-D-22-00235R1
Article Type:	Special Issue
Section/Category:	ICMMB
Keywords:	Additive Manufacturing; Arburg Plastic Freeforming; Patient-Specific Implants; PolyCarbonate Urethane
Corresponding Author:	Laura Cercenelli, Adjunct Professor, PhD Alma Mater Studiorum Universita di Bologna: Universita degli Studi di Bologna Bologna, ITALY
First Author:	Mattia Mele, PhD, Adjunct Professor
Order of Authors:	Mattia Mele, PhD, Adjunct Professor
	Laura Cercenelli, Ph.D., Adjunct Professor
	Gregorio Pisaneschi, PhD student
	Maurizio Fiorini, Associate Professor
	Andrea Zucchelli, Associate Professor
	Giampaolo Campana, Associate Professor
	Achille Tarsitano, Associate Professor
	Emanuela Marcelli, Associate Professor
Manuscript Region of Origin:	ITALY
Abstract:	Additive Manufacturing (AM) brings ground-breaking opportunities to provide customized healthcare solutions with reasonable time and cost. These benefits become more evident if reducing the distance between the printing process and surgery. In this direction, the Arburg Plastic Freeforming (APF) process offers unprecedented opportunities. The absence of hazardous feedstock materials such as powders allows for the utilization of this technology within hospitals. Also, unlike traditional AM processes, APF makes it possible to process medically approved standard granulates without compromising their certification. In this study, APF has been used to manufacture, for the first time, a patient-specific cranial implant (PSCI) using a biocompatible polymer with a high energy absorption capability, namely PolyCarbonate Urethane (PCU). The main technological issue was represented by the lack of a solvable support material compatible with PCU. This obstacle was overcome by a custom support structure made of the same material, which can be removed at the end of the process with limited damage to the PSCI. The orientation of the part within the building chamber was chosen to optimize the accuracy of critical features and the surface quality of the regions facing the brain. The 3D-printed cranial implant showed high toughness during mechanical impact tests.

3D PRINTING OF A CRANIAL IMPLANT WITH ENERGY-ABSORBING POLYMER VIA ARBURG PLASTIC FREEFORMING TECHNOLOGY

M. MELE[1], L. CERCENELLI[2]*, G. PISANESCHI[1], M. FIORINI[3], A. ZUCCHELLI[1], G. CAMPANA[1], A. TARSITANO[4,5], E. MARCELLI[2]

[1]*Department of Industrial Engineering, University of Bologna, Bologna, Italy*

[2]*eDIMES Lab-Laboratory of Bioengineering, Experimental Diagnostic and Specialty Medicine Department, University of Bologna, Bologna, Italy*

[3]*Department of Civil, Chemical, Environmental and Material Engineering, University of Bologna, Bologna, Italy*

[4]*IRCCS Azienda Ospedaliero Universitaria di Bologna, Oral and Maxillofacial Surgery Unit, Bologna, Italy, Bologna, Italy*

[5]*Department of Biomedical and Neuromotor Sciences, University of Bologna, Bologna, Italy*

**laura.cercenelli@unibo.it*

Additive Manufacturing (AM) brings ground-breaking opportunities to provide customized healthcare solutions with reasonable time and cost. These benefits become more evident if reducing the distance between the printing process and surgery. In this direction, the Arburg Plastic Freeforming (APF) process offers unprecedented opportunities. The absence of hazardous feedstock materials such as powders allows for the utilization of this technology within hospitals. Also, unlike traditional AM processes, APF makes it possible to process medically approved standard granulates without compromising their certification.

In this study, APF has been used to manufacture, for the first time, a patient-specific cranial implant (PSCI) using a biocompatible polymer with a high energy absorption capability, namely PolyCarbonate Urethane (PCU). The main technological issue was represented by the lack of a solvable support material compatible with PCU. This obstacle was overcome by a custom support structure made of the same material, which can be removed at the end of the process with limited damage to the PSCI. The orientation of the part within the building chamber was chosen to optimize the accuracy of critical features and the surface quality of the regions facing the brain. The 3D-printed cranial implant showed high toughness during mechanical impact tests.

Keywords: Additive Manufacturing, Arburg Plastic Freeforming, Patient-Specific Implants, PolyCarbonate Urethane

1. Introduction

Additive Manufacturing (AM) technologies offer unprecedented opportunities for the fabrication of Patient-Specific Implants (PSIs).

The main advantage of these processes over traditional moulding is the absence of fixed equipment, which makes the process easily adaptable to different geometries. Also, layer-by-layer fabrication allows for manufacturing complex structures that could not be obtained by machining. The AM has been recently introduced in various surgical fields, mainly including orthopaedics and maxillofacial surgery to manufacturing patient-specific tools, such as cutting

---

[*] Corresponding author

guides and customized implants that help to improve intraoperative accuracy and surgical outcomes [1–5].

In terms of materials, applications of AM to PSIs include both metals and polymers. The former category has been largely dominated by Titanium (Ti) alloys due to their biocompatibility, corrosion resistance, machinability and mechanical properties [6]. Nevertheless, the higher elastic modulus of Ti compared to human cortical bone often causes stress-shielding effects at the bone-implant interface. Moreover, the osteointegration of these materials is generally poor, requiring surface treatments to limit the risk of implant failures [7]. Bioceramics, such as bioactive glasses and calcium phosphates are advantageous over metals as they are more biocompatible and bioactive, although the low mechanical strength and the brittle nature make them inappropriate for load-bearing applications [8].

Recent research highlighted the opportunity to surpass these limitations through the adoption of polymeric materials. Specifically, Polyaryletherketone (PAEK) polymers like Polyetheretherketone (PEEK) and Polyetherketoneketone (PEKK) have gained popularity in dental and craniofacial reconstructions because of their biocompatibility, mechanical performance and chemical resistance [9,10]. Particularly, PEKK implants exhibited bone ingrowth, no fibrotic tissue formation, and significant increases in bony apposition over time due to the double ketone group that increases the ability of surface chemical modification leading to complex surface topography, greater surface area, and micro rough surface [11–13]. Another promising family of medical-grade polymers is represented by Polycarbonate Urethanes (PCUs). Current applications of these materials comprise neurostimulation, vascular, artificial heart, cardiac assist and diagnostic devices[14,15]. Because of their unique combination of toughness, durability, flexibility and biocompatibility, these polymers are used extensively in orthopaedic applications such as hip and knee joints and spinal motion preservation devices [14,16,17].

Formatted: Font co

Formatted: Font co

To date, the AM of polymers for PSIs has been mainly carried out by Laser Powder Bed Fusion (LPBF) and Fused Filament Fabrication (FFF) techniques [12,15,18]. LPBF is an efficient solution for the fabrication of porous and drug-releasing components. Nevertheless, this process poses some limitations as far as materials are concerned. Firstly, the range of semi-crystalline polymers processable through LPBF is limited by the need for a supercooling window to avoid part distortion while printing. Then, the powder-bed strategy means that the same material is found in all the regions of the part. Finally, powder management is questioned in a hospital environment regarding sterilization and safety [12]. The adoption of FFF processes is mainly fostered by the affordability of machines and the easy management of the feedstock material but its practical application is limited by several factors[19]. Particularly, filament production must preserve the medical compliance of the polymer, which affects the cost and the number of available materials. The number of manufacturable polymers is also limited by the requirements in terms of stiffness. On one hand, brittle materials may experience fragile breaking when the filament enters the deposition nozzle. On the other hand, elastomer-like materials are prone to buckling, which makes them unsuitable for this process[19,20]. FFF also suffers from limitations as far as the surface texture is concerned, since the dimension and shape of achievable details are constrained by the filament-based deposition strategy[21,22].

Arburg Plastic Freeforming (APF) is a novel AM technology offering the opportunity to surpass several of the limitations mentioned above[23]. This process melts granulate polymeric materials with a reciprocating screw similar to that use for the injection moulding process. A unique Droplet-Based (DB) deposition strategy is then used to build the three-dimensional part. A large number of medically approved standard granulates can be processed by APF technology into three-dimensional functional components, without compromising their certification. Moreover, it is possible to adopt several deposition nozzles to combine different materials within the same part. DB deposition also allows for more accurate control of surface textures if compared with FFF. This technology can be used in a cleanroom environment, which makes it particularly appealing for in-hospital applications. Previous studies demonstrated the opportunity to realize drug-releasing medical devices via APF[24]. To date, there are very limited studies investigating the properties of medical-grade polymers processed via APF[25].

This study investigates the opportunity to manufacture a patient-specific cranial implant using APF 3D printing technology and a biocompatible polymer with a high energy absorption capability, namely PCU. Preliminary conclusions are drawn from quasi-static and dynamic mechanical tests carried out on a 3D-printed PCU cranial plate.

2. Materials and Methods

2.1. Case study

The human head may undergo impact loads leading to skull fracture or other injuries that require the removal of part of the skull. Consequently, the removed portion is replaced using autologous bone or alloplastic material, named cranial plate. In this paper, a customised cranial plate for a patient who suffered from a severe accident was used as a case study. The patient (a 49 year-old caucasian female) was already treated at the Oral and Maxillofacial Surgery Unit of IRCCS Azienda Ospedaliero Universitaria di Bologna by the implantation of a custom-made cranial plate manufactured in biocompatible PEEK using SLS 3D printing technology. The customised design of the PSCI obtained as described in the next sections, is used as a base for this study.

2.2. PSCI design

The process started with the acquisition of computed tomography (CT) scan of a patient trauma head. Image segmentation was performed using Mimics Medical software (Materialise, NV, Leuven, Belgium). A threshold-based segmentation was mainly used for the identification of the skull bones. Then, a 3D-reconstructed model of the pre-operative patient skull was obtained and exported in the STL format [Fig.1a]. The resulting segmentation and 3D digital model of the patient's skull were accurately checked and approved by the surgeons. Starting from this skull model, the cranial implant dimension and contour were extracted, and the patient-specific reconstructive plate was designed in order to ensure the perfect matching of the implant to the host skull geometry, using 3-Matic software (Materialise NV, Leuven, Belgium) [Fig.1b]. The PSCI has a surface area of 147 cm^2, a volume of 23 cm^3 and a thickness of 4 mm, degrading to approximately 1 mm along the edges at the interface with the skull [Fig.1b].

Formatted: Supersc

Formatted: Supersc

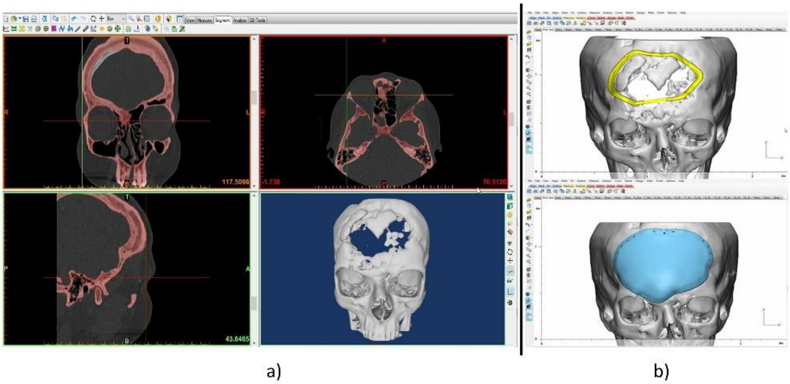

Fig. 1: Segmentation masks and 3D-reconstructed model of the post-trauma patient skull (a). Virtual design of the patient-specific reconstructive plate (b).

2.3. *PCU material*

Pellets of amorphous thermoplastic medical grade PCU (Bionate® 75D PCU, DSM Biomedical Inc., Berkeley, CA, USA) were used for this investigation. Bionate® 75D PCU is a medical-grade polymer suitable for use in long-term implants[16].

Formatted: Font co

Due to its physical and mechanical properties (Tab.1, Datasheet: *available at https://www.dsm.com/content/dam/dsm/biomedical/en_us/documents/document-bionate-pcu-productsheet.pdf*), the Bionate® 75D PCU material can be considered an excellent candidate for investigating AM fabrication of maxillofacial PSI as the one investigated in this study.

Tab. 1 – Main physical and mechanical properties of Bionate® 75D PCU

Property	**Value**
Hardness, Shore D	73D
Ultimate Tensile Strength	63.23 MPa
Ultimate Elongation	241%
Flexural Modulus, 1% Secant Modulus	1792.6 MPa
Flexural Stress, at 5% Deflection	70.3 MPa
Recommended Extrusion Conditions	190°C-232°C

2.4. 3D printing of PSI using APF technology

An Arburg Freeformer 2X-200K printer (Arburg GmbH, Lossburg, Germany) was used to fabricate the designed cranial plate. A schematic representation of the APF printing process is shown in Fig.2.

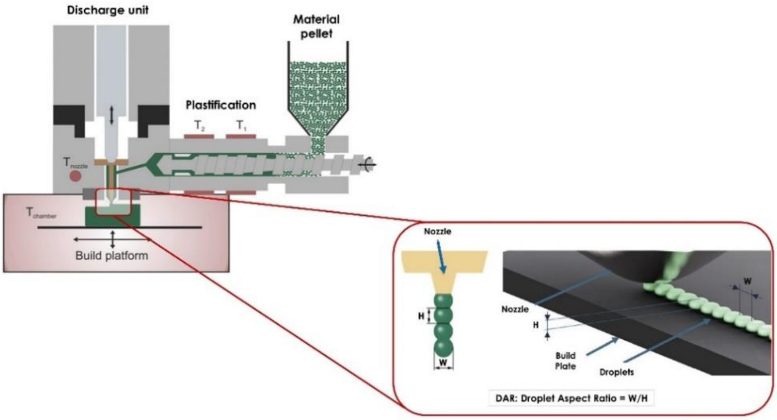

Fig.2: Arburg Plastic Freeforming (APF) printing process.

The APF technology is an open system meaning that variations of several process parameters are allowed to allow the processing of third-party materials. For this study, printing settings were identified starting from a set of parameters suggested by Arburg. An optimization was made by varying the Drop Aspect Ratio (DAR, see Fig.2) and the nozzle temperature[26]. Specifically, the DAR was adjusted so as to achieve accuracy, avoiding over or under-filling on benchmark parallelepipeds of 20 mm x 20 mm x 5 mm. The nozzle and chamber temperatures were chosen so as to increase the layer adhesion and prevent material degradation. The resulting printing parameters used for the present study are summarised in Tab.2.

Tab. 2 - Printing parameters used for processing PCU by APF

APF Printing parameters for Bionate PCU	
Nozzle Temperature [°C]	230
Zone 1 Temperature [°C]	225
Zone 2 Temperature [°C]	180
Chamber Temperature [°C]	120
Drop Aspect Ratio (DAR)	1.3
Contour speed [mm/s]	15
Hatching speed [mm/s]	60

Infill direction [°]	±45
Contour lines	2
Infill percentage [%]	100
Contour overlap [%]	50

The designed cranial plate was oriented for printing with the loaded surface facing the building plate (Fig. 3). Due to the surface curvature, support structures are necessary for printing. To date, no experience with solvable APF printed support materials compatible with PCU has been reported. Consequently, support structures were realised using the same PCU material and mechanically removed at the end of the printing job. Two replicas of the cranial plate were manufactured using different infill percentages for the support structures, namely 25% (PCU_25%) and 50% (PCU_50%).

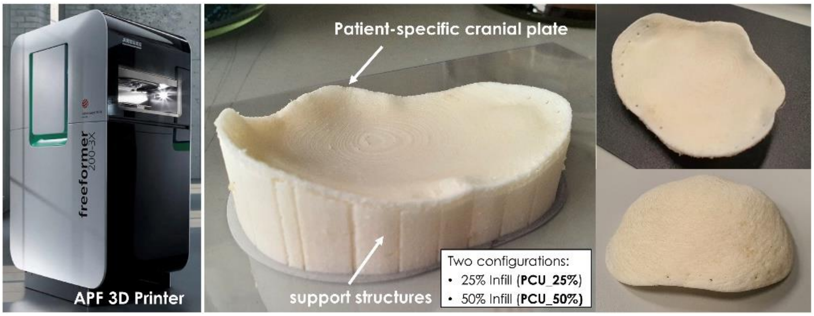

Fig. 3: The 3D printed PCU cranial plate using APF technology. Two configurations having different infill percentage (PCU_25% and PCU_50%), were manufactured and tested.

2.5. *Experimental phase*

2.5.1. *Static compressive load tests*

The static compressive load tests were carried out on an INSTRON electro-mechanical Universal machine equipped with a 10 kN load cell, at a 2mm/min speed. The load measurement accuracy (class 0.5) is ± 0.5% of reading down to 1/1000th of the load cell's capacity. Therefore, with a load of 10 N the accuracy is ± 0.05 N. To anchor the cranial plate to the testing machine, a support base was manufactured in carbon fibre-reinforced polyamide PAHT CF15 using a Prusa i3 MK3 3D printer, and the plate was mounted on it with surgical screws. Then the support base was anchored to a metallic base positioned on the testing machine (Fig.4). Static loads were applied at the centre of the implant, and the test ended when a maximum vertical displacement of 6 mm was reached.

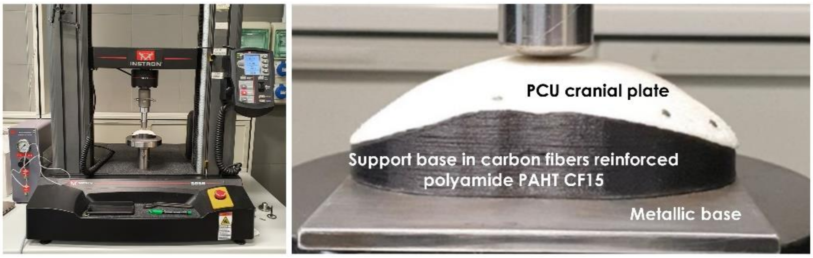

Fig. 4: Set up for the static compressive load tests on the 3D-printed PCU cranial plate.

2.5.2. *Impact tests*

Drop weight impact testing is used to measure the energy absorption of the obtained 3D-printed PCU plates under dynamic loads.

A drop weight impact testing machine available at the Mechanical Engineering Laboratory of the University of Bologna was used for the tests (a detailed description of it can be found in [27]). The metal base, to which the cranial plate is anchored, is centred using reference pins and fixed to the base of the machine platform by means of four clamps. The part is positioned so that the punch hits the cranial plate in its centre (Fig.5). The punch (impactor) is connected to the mobile crosspiece which can slide vertically on two guides and is suspended using an electrically operated magnet.

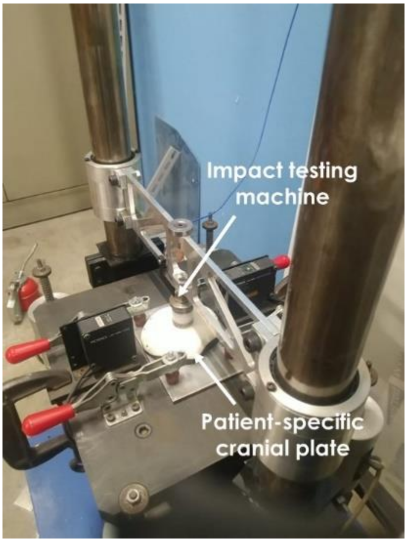

Fig. 5: Set up for the impact tests on the 3D-printed PCU cranial plate.

In the impact phase, the punch displacement is measured through a laser beam: when the punch is in the rest position the laser beam records a constant voltage. When the punch enters the beam window, the voltage decreases to a minimum

Formatted: Indent:

value when the beam is completely covered by the punch. The detected electrical signal is then converted into displacement by means of fine-tuned empirical coefficients. The force values are recorded by a piezoelectric sensor (PCB, Model 208C05) placed between the punch and the crosspiece structure. The drop tower test works with an impact force from 40 N to 20 kN, 100 kHz frequency of acquisition, and an accuracy ± 0.1 N.

Formatted: Not Hig

Starting from this data, a map of displacement, speed and accelerations during the whole impact phase is obtained. For each 3D-printed cranial plate (PCU_25%, PCU_50%), the tests were performed with an increasing height of the impactor (drop height) until the part was broken or damaged. It was decided to start with an impact energy of about 2 J and increase in steps of about 2 J, up to a value that caused the first sign of failure (i.e. impact energies from 2 J up to about 16 J).

3. Results

3.1. Results of static compressive load tests

The obtained load-displacement curves are reported in Fig.6. Both 3D-printed plate configurations showed a high vertical displacement for rather low applied static loads (< 500 N). A detailed view of the vertical displacement achieved for the two plates at a static load of 50 N is reported in Fig.7.

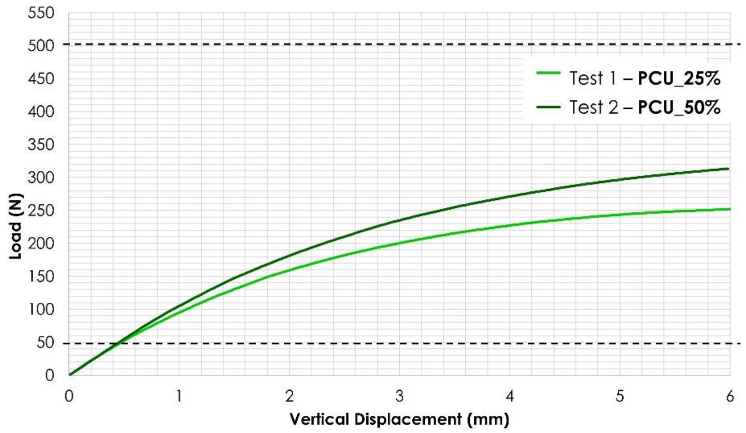

Fig. 6. Load-displacement curves obtained for the two 3D-printed plates having different infill percentages for the supporting structures (PCU_25%, PCU_50%).

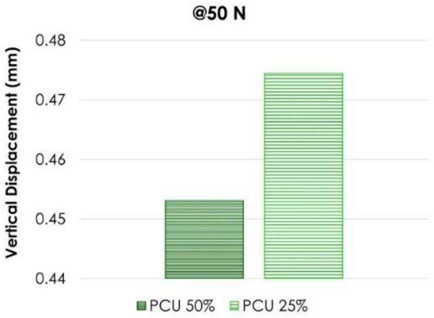

Fig.7. Vertical displacement of two 3D-printed plates (PCU_25%, PCU_50%) and the nominal PCU displacement, for 50N test load condition.

3.2. *Results of impact tests*

In all tests, the punch rebounded on the PCU plate following the impact, until the last test carried out for each implant, in which a sign of breaking was detected, and the tests were stopped. In fact, in test 8 for PCU_25% and test 10 for PCU_50%, a crack has arisen nearby one of the screw holes. This crack propagates towards the outer edge of the plate. However, the parts resisted the impact, demonstrating a great energy absorption capacity by PCU material.

Figures 8 and 9 show the force-displacement curves relating to the impact tests performed with the two PCU cranial plates (PCU_25%, PCU_50%). The recorded values for maximum displacement, maximum force and absorbed energy are reported in Tables 3 and 4, together with the drop height, the impact speed and the impact energy. In Figure 10, the maximum displacement, the maximum force and the absorbed energy of both implants are compared for different heights of fall (tests 1 to 10 with the respective height of 0.14 m to 1.40 m).

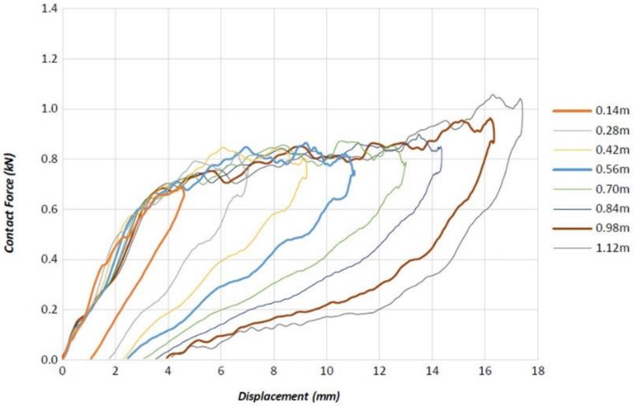

Fig.8. Force-displacement curves for PCU_25% cranial plate, for each tested drop height.

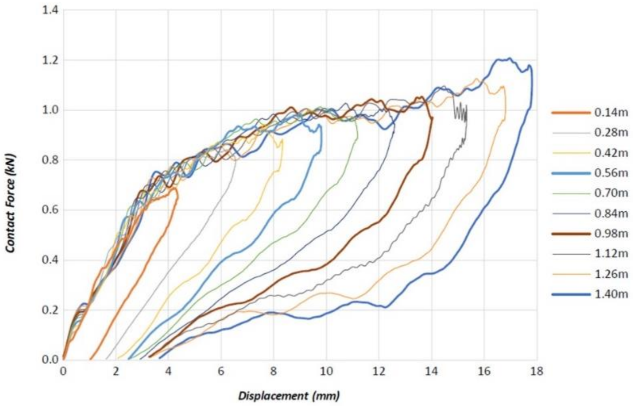

Fig.9. Force-displacement curves for PCU_50% cranial plate, for each tested drop height.

Tab. 3 – Results of impact tests performed on PCU_25% cranial plate, for each tested drop height.

PCU_25%						
Test	**Drop Height [m]**	**Impact speed [m/s]**	**Impact Energy [J]**	**Absorbed Energy [J]**	**Maximum Displacement [mm]**	**Maximum Force [kN]**
1	0.140	1.70	2.13	0.99	4.60	0.687
2	0.280	2.40	4.26	2.29	7.05	0.826
3	0.420	2.91	6.29	3.66	9.25	0.847
4	0.560	3.25	7.82	4.71	11.05	0.865
5	0.700	3.65	9.83	6.34	13.00	0.872
6	0.840	3.89	11.20	7.59	14.36	0.900
7	0.980	4.26	13.43	9.54	16.34	0.963
8	1.120	4.44	14.59	10.80	17.42	1.057

Tab. 4 – Results of impact tests performed on PCU_50% cranial plate, for each tested drop height.

PCU_50%						
Test	**Drop Height [m]**	**Impact speed [m/s]**	**Impact Energy [J]**	**Absorbed Energy [J]**	**Maximum Displacement [mm]**	**Maximum Force [kN]**
1	0.140	1.64	1.99	0.96	4.35	0.6905
2	0.280	2.32	3.98	2.10	6.56	0.8417
3	0.420	2.83	5.91	3.35	8.34	0.9419
4	0.560	3.16	7.39	4.36	9.81	0.986
5	0.700	3.48	8.96	5.51	11.19	1.0132
6	0.840	3.77	10.52	6.66	12.60	1.0276
7	0.980	4.10	12.44	8.15	14.03	1.0534
8	1.120	4.35	14.00	9.55	15.33	1.0967
9	1.260	4.62	15.79	11.12	16.81	1.1265

10	1.400	4.79	16.94	12.43	17.82	1.2075

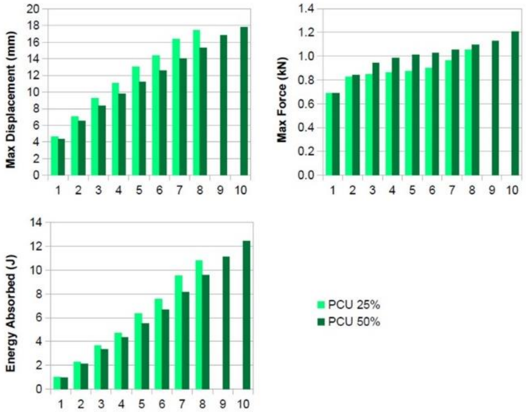

Fig.10. Comparative results for maximum displacement, maximum contact force, and absorbed energy between the two printed PCU plates.

4. Discussion

In this paper, the APF printing technology was applied for the first time to produce a patient-specific cranial implant in Bionate PCU material. APF has been selected because it offers the capability to process medical-grade plastics in the form of pellets. In terms of medical application, the processing of granules offers a considerable advantage since no further filament-making is necessary. Thus, no further manufacturing step has to be certified for medical purposes.

The APF technology is an open system meaning that variations of almost all process parameters are allowed by the user. This flexibility results in a great variety of processable materials, but it also means that the processing parameters have to be identified by the user. Process parameter optimization is a complex task since these interactions are not yet well understood. Thus, the material qualification or optimization of the mechanical properties of new materials has to be done systematically.

For this study, a medical-grade Bionate 75D PCU was chosen. This material is totally new as far as the processing of cranial implants with APF is concerned. For this reason, an extensive research effort is required for parameter optimization, such as temperature profile along the reciprocating screw, melt pressure and nozzle temperature in order to ensure good droplet deposition. However, PCU is easier to process due to the lower crystallinity and lower processing temperature than other technical polymers relevant to medical applications, like PEEK and PEKK, that need a high-temperature 3D printer machine, with a considerably increased complexity in the process management.

In this study, we achieved a good printability of Bionate 75D PCU material with the identified APF printing parameters. Surely, there is still room for improving the mechanical performance of the 3D-printed PCU part, as demonstrated by our results.

Indeed, the poor performance of the 3D-printed cranial plate was observed when subjected to static compressive loads. If we consider previous studies in the literature, two static load conditions can be taken as reference for the cranial implant use case: the first condition (50 N) approximates the reaction force induced on the skull when resting on a flat surface without any other external force acting on it[28]; the second load (500 N) simulates a scenario in which the implant undergoes a real impact of heavy weight or vehicle[29]. Static compressive load tests performed on the two printed PCU plates demonstrated that both resist at 50 N. However, they cannot withstand high loads as those expected in the worst-case scenario of a real heavy impact since a 500 N load is not reached even at high displacements. This means that the printing process significantly affects mechanical behaviour. This loss of mechanical proprieties might be explained by a not optimal adhesion of the drops or generation of some voids during the printing process.

For the study, the Arburg Freeformer 2X-200K printer, having a chamber temperature which hardly reaches 120°C, was used. It would be interesting for future studies to print some cranial plates with the APF 300-3X machine which offers a higher chamber and nozzle temperature, and then evaluate the achieved mechanical performance for those parts. In general, the mechanical resistance of the printed plate resulted critical due to the curved shape and the lack of full support, which surely introduces a decrease in material adhesion and mechanical proprieties. The compressive test outcomes were relevant for understanding the effect of the different infill percentages for the support structures. Indeed, results showed that the cranial plate printed with a less dense support structure (PCU_25%) bears less load at a given value of displacement than the PCU_50% (Fig.6) and exhibited the greatest deformation (Fig.7).

~~In this study, the same PCU material has been used to print the plate and the supports, since no previous experience on solvable APF printed support materials compatible with PCU has been reported. Future efforts should be addressed to investigate and experiment with the combined use of PCU and solvable support materials, such as PVA and PVP, in the APF printing process. The choice of optimal support material is essential, since removing support made with the same PCU material is quite critical and surely compromises both the mechanical performance and the surface finishing of the part.~~

The most interesting result of the study was the high energy absorption capacity of the PCU cranial plate. These findings agree with previous observations on Bionate PCU material[18] reporting an interesting elastomeric behaviour that can help to absorb impact energy and avoid stress concentration. Indeed, looking at the obtained force-displacement curves (Fig. 8, 9) large displacements of the printed part can be observed when it is subjected to dynamic load conditions (i.e. impact with the falling punch). In all curves, it is possible to distinguish a first phase in which the force increases. This portion of the curve corresponds to the phase in which the punch descends, deforming the plate. In the second phase, the force decreases and the punch rises under the effect of the rebound. All curves showed a large area between the ascending and descending sections of the curves. This area represents the energy dissipated in the impact phase which is absorbed by the PCU material.

Linear force increase may be seen at the beginning of the curve for each trial. The force then starts to build more slowly and less linearly, and the bigger the impact energy, the longer the stretch of the curve. The vibrations of the testing machine cause some of the apparent oscillation; the same effect was clearly noticed in[30]. The fact that the initial half of the curve is linear and consistent across tests indicates that following absorption of the impact energy, even with large plate deformations of up to 18 mm, the plate's behaviour was always reversible.

Because the initial linear segment maintains the same slope even after being impacted, the component has not undergone irreversible deformation. It exhibits nonlinear but reversible behaviour as a result. This might be related to two factors: the material having elastomer-like behaviour, and the geometry being shell-like, which can undergo buckling phenomena by transitioning from shell-like to plate-like behaviour, resulting in nonlinear yet reversible behaviour.

In Fig.10 it can be observed that the implant PCU 25% sustained higher displacements and correspondently absorbed more energy, due to its higher compliance related to the presumably lower density. For this reason, the 50% PCU resisted a higher level of force and impact energy. In both cases, the growth of the maximum force, after initial growth, began to settle down until the last tests in which it started to grow again until the plate failed.

In some ways, it may be significant to have found a good dynamic behaviour of the material rather than a high mechanical performance in static conditions. This means that the printed PCU material is able to internally redistribute the load it undergoes during the impact by absorbing the energy without reaching the failure. This may be beneficial to preserve the integrity of the prosthesis after implantation in case it is subjected to dynamic loads, and limits the stress concentration on critical points such as screw holes.

Study limitations

In the study the same PCU material has been used to print the plate and the supports, since no previous experience on solvable APF printed support materials compatible with PCU has been reported. This surely compromises both the mechanical performance and the surface finishing of the printed plate, since removing the supports made with the same PCU material is quite critical. Future efforts should be addressed to investigate and experiment with the combined use of PCU and solvable support materials, such as PVA and PVP, in the APF printing process.

In the study we considered a single geometry for the PSCI, which was originally designed for PEEK material. Significant improvements in maximum deformation and stress could be undoubtedly achieved by optimising the cranial plate design for PCU. For example, small variations in the plate thickness may considerably affect the mechanical response of the part.

Formatted: Indent:

The present investigation is ~~based~~ limited only ~~on~~ to experimental tests. To properly assess the potential of new 3D-printed PCU patient-specific implants, it could be useful to associate this experimental study with a computational modelling study. Computational mechanics allow for simulating the loading conditions for the implant and to understand which are the most critical points for mechanical failure. This information may help to further optimize the printing process, e.g. to define the most appropriate part orientation, and the implant design.

5. Conclusion

Arburg Plastic Freeforming (APF) has been successfully applied for the first time to manufacture a patient-specific cranial implant using a medical-grade polycarbonate urethane (PCU) copolymer. Static tests highlighted severe deformations of the implant even for moderate loads. On the other hand, PCU demonstrated a high capacity to absorb energy in case of impacts, thus allowing for preserving the integrity of the prosthesis. These findings suggest that the material has great potential for applications in craniomaxillofacial prostheses which may undergo impacts during their life.

The opportunity to carry out the manufacturing via APF opens new opportunities for the fabrication of customized devices in hospital environments. Nonetheless, the results also highlight the need for careful optimization of the printing process. Particularly, it was demonstrated that the support structures have relevant influence on the quasi-static and dynamic mechanical properties of the implant. Further research should thus be devoted to identifying solvable support materials compatible with the APF printing of PCU so as to allow for producing full support structures.

References

1. Zaffagnini, S. *et al.* Custom-Made Devices Represent a Promising Tool to Increase Correction Accuracy of High Tibial Osteotomy: A Systematic Review of the Literature and Presentation of Pilot Cases with a New 3D-Printed System. *J Clin Med* **11**, 5717 (2022).
2. Aman, Z. S. *et al.* Improved Accuracy of Coronal Alignment Can Be Attained Using 3D-Printed Patient-Specific Instrumentation for Knee Osteotomies: A Systematic Review of Level III and IV Studies. *Arthroscopy* **38**, 2741–2758 (2022).
3. Tarsitano, A. *et al.* Accuracy of CAD/CAM mandibular reconstruction: A three-dimensional, fully virtual outcome evaluation method. *Journal of Cranio-Maxillo-Facial Surgery: Official Publication of the European Association for Cranio-Maxillo-Facial Surgery* **46**, 1121–1125 (2018).
4. Battaglia, S. *et al.* Computer-assisted surgery for reconstruction of complex mandibular defects using osteomyocutaneous microvascular fibular free flaps: Use of a skin paddle-outlining guide for soft-tissue reconstruction. A technical report. *J Craniomaxillofac Surg* **47**, 293–299 (2019).
5. Battaglia, S. *et al.* Combination of CAD/CAM and Augmented Reality in Free Fibula Bone Harvest. *Plast Reconstr Surg Glob Open* **7**, e2510 (2019).

Formatted: Italian (

6. Niinomi, M. Mechanical biocompatibilities of titanium alloys for biomedical applications. *J Mech Behav Biomed Mater* **1**, 30–42 (2008).
7. Zhang, J. *et al.* Promoting osseointegration of titanium implants through magnesium- and strontium-doped hierarchically structured coating. *Journal of Materials Research and Technology* **16**, 1547–1559 (2022).
8. van Gestel, N. a. P. *et al.* Clinical Applications of S53P4 Bioactive Glass in Bone Healing and Osteomyelitic Treatment: A Literature Review. *Biomed Res Int* **2015**, 684826 (2015).
9. Alqurashi, H. *et al.* Polyetherketoneketone (PEKK): An emerging biomaterial for oral implants and dental prostheses. *J Adv Res* **28**, 87–95 (2021).
10. Dua, R., Rashad, Z., Spears, J., Dunn, G. & Maxwell, M. Applications of 3D-Printed PEEK via Fused Filament Fabrication: A Systematic Review. *Polymers (Basel)* **13**, 4046 (2021).
11. Adamzyk, C. *et al.* Bone tissue engineering using polyetherketoneketone scaffolds combined with autologous mesenchymal stem cells in a sheep calvarial defect model. *J Craniomaxillofac Surg* **44**, 985–994 (2016).
12. Basgul, C., Spece, H., Sharma, N., Thieringer, F. M. & Kurtz, S. M. Structure, properties, and bioactivity of 3D printed PAEKs for implant applications: A systematic review. *J Biomed Mater Res B Appl Biomater* **109**, 1924–1941 (2021).
13. Banerjee, K., Debroy, M., Balla, V. K. & Bodhak, S. Recent progress in 3D-printed polyaryletherketone (PAEK)-based high-performance polymeric implants for musculoskeletal reconstructions. *Journal of Materials Research* **36**, 3877–3893 (2021).
14. Elsner, J. J. & McKeon, B. P. Orthopedic Application of Polycarbonate Urethanes: A Review. *Techniques in Orthopaedics* **32**, 132–140 (2017).
15. Araujo Borges, R., Choudhury, D. & Zou, M. 3D printed PCU/UHMWPE polymeric blend for artificial knee meniscus. *Tribology International* **122**, 1–7 (2018).

Formatted: Font co

16. Geary, C., Birkinshaw, C. & Jones, E. Characterisation of Bionate polycarbonate polyurethanes for orthopaedic applications. *J Mater Sci Mater Med* **19**, 3355–3363 (2008).
17. van Tienen, T. G., Hannink, G. & Buma, P. Meniscus replacement using synthetic materials. *Clin Sports Med* **28**, 143–156 (2009).
18. Idà, E., Nanetti, F. & Mottola, G. An Alternative Parallel Mechanism for Horizontal Positioning of a Nozzle in an FDM 3D Printer. *Machines* **10**, 542 (2022).
19. Campana, G., Mele, M., Ciotti, M. & Rocchi, A. Environmental impacts of self-replicating three-dimensional printers. *Sustainable Materials and Technologies* **30**, e00335 (2021).
20. Kumar, B. P., Venkatesh, V., Kumar, K. A. J., Yadav, B. Y. & Mohan, S. R. Mandibular Reconstruction: Overview. *J Maxillofac Oral Surg* **15**, 425–441 (2016).
21. Ciotti, M., Campana, G. & Mele, M. A review of the accuracy of thermoplastic polymeric parts fabricated by additive manufacturing. *Rapid Prototyping Journal* **28**, 358–389 (2021).
22. De Bernardez, L. *et al.* Effects of infill patterns on part performances and energy consumption in acrylonitrile butadiene styrene fused filament fabrication via industrial-grade machine. *Prog Addit Manuf* (2022) doi:10.1007/s40964-022-00316-4.
23. Mele, M., Campana, G. & Fumelli, G. Environmental impact assessment of Arburg plastic freeforming additive manufacturing. *Sustainable Production and Consumption* **28**, 405–418 (2021).
24. Welsh, N. R., Malcolm, R. K., Devlin, B. & Boyd, P. Dapivirine-releasing vaginal rings produced by plastic freeforming additive manufacturing. *Int J Pharm* **572**, 118725 (2019).
25. Hentschel, L., Kynast, F., Petersmann, S., Holzer, C. & Gonzalez-Gutierrez, J. Processing Conditions of a Medical Grade Poly(Methyl Methacrylate) with the

Formatted: Font co

Arburg Plastic Freeforming Additive Manufacturing Process. *Polymers* **12**, 2677 (2020).

26. Mele, M., Pisaneschi, G., Campana, G., Zucchelli, A. & Ciotti, M. Effect of selected process parameters on dimensional accuracy in Arburg Plastic Freeforming. *Rapid Prototyping Journal* **28**, 1677–1689 (2022).
27. Brugo, T. M. *et al.* Self-sensing hybrid composite laminate by piezoelectric nanofibers interleaving. *Composites Part B: Engineering* **212**, 108673 (2021).
28. Ridwan-Pramana, A. *et al.* Structural and mechanical implications of PMMA implant shape and interface geometry in cranioplasty – A finite element study. *Journal of Cranio-Maxillofacial Surgery* **44**, 34–44 (2016).
29. Wan, Z., Huang, C., Li, Y., Wan, C. & Zhong, R. The evaluation of bio-mechanical properties of four different skull implants by finite element methods. *Biomedical Research (India)* **29**, 1879–1884 (2018).
30. Zarei, H. *et al.* Low velocity impact damage assessment of GLARE fiber-metal laminates interleaved by Nylon 6,6 nanofiber mats. *Composite Structures* **167**, 123–131 (2017).